ISBN: 978-628-95207-8-1. ISSN: 2414-6390. Digital Object Identifier: 10.18687/LACCEI2024.1.1.1954

Design and Simulation of Integrated Distributed Energy Resources onto the Island of Saint Lucia

Phillip Polselli, MSEE and Pritpal Singh, PhD
[1]Department of Electrical and Computer Engineering, Villanova University, USA, ppolselli.stem@gmail.com, Pritpal.singh@villanova.edu

Abstract*— This study examines the current generation capacity and load demand of the Caribbean island of Saint Lucia. A 2015 national energy transition plan published by the utility company on Saint Lucia details the necessary expansion into solar and wind resources to decrease reliability on imported fossil fuels while maintaining proficient grid reliability. Presently, about 5% of total generation capacity can be supplied through distributed solar resources. The goal of this investigation is to determine site locations around the island which have ideal conditions for distributed energy resource (DER) development. Typical meteorological data analysis of solar irradiance and wind speed was performed to characterize the generation capacity and performance of the proposed DERs. These grid-connected DERs were simulated using ETAP modelling software to determine generation contribution to a substation in a distribution network. The results from this simulation yielded that the two proposed DER installations could supply 11.91% of total grid demand on a typical day. Further analysis strongly suggests that wind powered DERs are significantly advantageous due to consistent wind speeds throughout the year.

Keywords-- List at most 5 key index terms here.

I. INTRODUCTION

Over the past few decades, both the demand for energy and its societal reliance have increased drastically. It is estimated in 2019, that 78.91% of global electric consumption was sourced by fossil fuels. [1] This global over-reliance on fossil fuels causes environmental harm and economic dependence on the importation of fossil fuels. Both impacts are significant for small island developing states (SIDS). These islands are generally reliant on tourism for income. Therefore, negative impacts toward the island's environment or an increased cost of energy can result in reduced economic output. To mitigate these concerns, distributed energy resources (DERs) should be implemented to secure energy independence and cut carbon emissions from conventional energy sources. In this paper we explore the opportunities for expanding renewable energy implementation on the Caribbean Island of St. Lucia.

A. St. Lucia Background

Saint Lucia is an island located in the southern Caribbean Sea approximately 375 km off the northern coast of Venezuela. The island is approximately 620 km^2 and has an estimated population of 185,000. [2][3] The island has designated 18.7% of its terrestrial land as protected wildlife areas. [4] These wildlife areas and tropical climate are primary tourist attractions. The tourism industry is crucial for the economy of Saint Lucia, as it provides employment for 81.7% of the total workforce, and accounts for 65% of the nation's gross domestic product (GDP). The total GDP being 2.65 billion U.S dollars (USD), with an estimated tourism contribution of 1.723 billion USD. [5] In addition to significant reliance on tourism. St. Lucia is also heavily dependent on foreign energy imports. Presently, Saint Lucia spends approximately 10% of its GDP on fuel imports, which also comprises 18% of its total import of goods. [6] Since 2000, the average consumption of diesel fuel for electricity generation has increased by 1.47% annually.

B. Current Saint Lucia Power Generation and Distribution

Presently, nearly all electricity generation is supplied by a single electric utility provider known as LUCELEC. There is a single power generation station located in the most populous district of Castries. The Cul-de-Sac Power Station (CDSPS) currently employs a fleet of ten diesel generators. [7] When CDSPS was commissioned in 1990, it consisted of three 7 MW MAK diesel generators. Over time, LUCELEC has integrated higher capacity Wärtsilä diesel generators. Table 1 lists the composition of the generator fleet.

TABLE 1: CDSPS Generator Fleet

Manufacturer	Quantity	Total Generation Capacity (MW)
MAK	3	20.67
Wärtsilä	4	37.20
Wärtsilä	3	30.60

The total generation capacity of CDSPS is 88.4 MW. The peak demand reported in 2021 is 60.92 MW. LUCELEC utilizes a 66 kilovolt (kV) transmission system and an 11 kV distribution system to supply power to seven substations. [8] A comparison of generation capacity to peak demand shows there is 27.48 MW of unutilized generation. However, the Electricity Supply Act of 2008 implemented an edict which dictated a new set of operational guidelines for LUCELEC.

Specifically, clause 27.1 requires that sufficient generation capacity is available if the two largest generation units are unavailable. [9] Therefore, the firm capacity is defined as 68 MW. Based on the expected annual peak demand growth, it is estimated that clause 27.1 will be broken by 2026. Since 2015, the government of Saint Lucia has defined a National Energy Transition Strategy (NETS) focused on obtaining reliable, stable, and clean energy resources.

C. Saint Lucia National Energy Transition Strategy

In 2015, Saint Lucia began its National Energy Transition Strategy (NETS) with the primary goal to increase renewable energy penetration to 38.9% by 2025. [10] The proposed mix of renewable resources would include centralized solar and wind installations, complemented by energy storage devices. During 2015, the proposed capacities of these technologies were 54 megawatts (MW) of solar, 18 MW of wind, and 27 megawatt-hours (MWh) of energy storage.[10] In 2018, a 3 MW fixed-tilt photovoltaic (PV) installation was commissioned at Vieux Fort, located at the southern-most part of the island. A photograph of this plant is shown in Figure 1. As of 2022 the Vieux Fort PV installation had produced 24.7 MWh of electricity, which represents a 1.27 million Imperial gallon (gal) fuel reduction. [11] Additionally, there are 174 roof-mounted solar installations around Saint Lucia which contribute a generation capacity of 1.49 MW. [11] Comparing the current renewable energy portfolio to the NETS goal presented in 2015, the renewable energy integration process requires appreciable planning and funding. Nevertheless, Saint Lucia is committed to growing its renewable energy portfolio.

Significant improvements to the power distribution infrastructure of Saint Lucia are currently being implemented. The Vieux Fort PV installation is being expanded to have a generation capacity of 7.5 MW, with the new addition of a 3 MWh battery storage system. [11] Additionally, there are plans to construct a 10 MW PV installation with an energy storage element onto the east coast of the island; however, the exact location has not been disclosed. [11] Furthermore, there are goals to construct and integrate a 12 MW wind power installation in the Dennery district on the eastern side of Saint Lucia. The planned integration of these DERs has led LUCELEC to retrofit its grid with new fiber optic communication systems to meter and monitor load generation, consumption, and faults. [11] Summing the rated capacity of these proposed DERs yields 29.5 MW of generation capacity and at least 3 MWh of battery storage. Due to the substantial investment required to design and commission these renewable energy resources, it is imperative to understand the advantages of each technology, as well as to utilize as much existing infrastructure as possible.

Figure 1: Vieux Fort Solar Array Installation [12]

II. PV AND WIND SITE SELECTIONS

A. Centralized Photovoltaic Installation Site Selection

The site location selection for utility-scale centralized solar power installations is paramount to ensuring long term operation and success. Exposure to solar irradiance is the primary design driver in solar power system installation. Preliminary searches around the eastern side of Saint Lucia yielded a few locations which are advantageous for centralized solar installations, primarily due to relatively flat land and limited shading obstructions. Both potential sites are in the Desruisseaux region, located on the southeast side of the island. Shown in Figure 2 is a site located close to the coast. This site is advantageous since its gradient is near zero, and it is already located near 11 kV distribution lines.

Figure 3 is a potential site located inland. This plot is larger than the coastal region and has a low gradient ranging between 1% and 5.16%. [13][14] Initial comparison of these two sites would suggest that the coastal location is more suitable due to its proximity with the island's 11kV distribution system. However, this site is at an increased risk for flooding and naturally more prone to tropical storms. Due to this risk, it is assumed that additional design measures would need to be integrated into the power conversion equipment and cable ways, resulting in higher design, installation, and preventative maintenance costs. In contrast, the inland location offers a higher elevation which eliminates all risk of flooding but introduces a few other disadvantages. The disadvantages being increased array design cost due to an uneven land gradient, increased distribution line length, and an increase in shading obstructions. These disadvantages result in an increase in upfront cost for the design of the system but should not result in an increase in cost for periodic maintenance.

Figure 2: Potential PV Site Desruisseaux Coastal [13]

Figure 3: Potential PV Site Desruisseaux Inland [13]

The chosen locality is ideal for a centralized PV installation. The estimated gradient of the land is south-sloping 3.03%. [14] This slight gradient is advantageous for PV installation, since it will aid to reduce shading caused by neighboring rows of PV modules. The PV modules are installed onto a freestanding structure, which elevates the modules 0.60 m above the ground to permit sufficient cable management, site maintenance, and wind convection. Each row in the array supports two PV modules with a collector tilt angle of 15° and an azimuth angle of 0°. This collector tilt angle was chosen to complement the latitude of Vieux Fort; doing such maximizes the direct beam insolation (IBC) incident onto the face of the PV modules. Typical-meteorological-year (TMY) data published by NREL in 2020, through the National Solar Radiation Database (NSRDB), was utilized to quantify the expected total incident insolation and the expected power supplied by the Vieux Fort array. [15] Figure 4, shows the total incident insolation onto the face of the PV modules between the hours of 5:30 AM and 6:30 PM on the 21st day of each month of the year.

Table 2: TSM 245 DC-05 Temperature Specification

Specification	Data Sheet Rating
Open Circuit Voltage (α)	-0.45% / °C
Short Circuit Current (β)	0.05% / °C
Maximum Power (γ)	-0.35% / °C

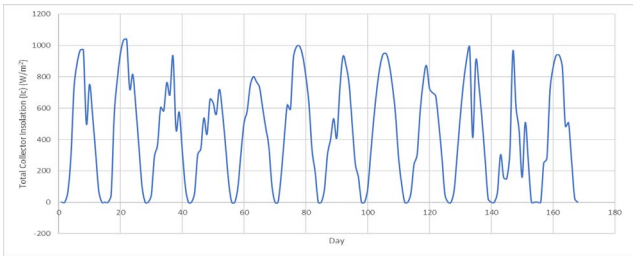

Figure 4: Vieux Fort Insolation on the 21st day of each month

The solar insolation does not vary greatly from month to month as expected due to Saint Lucia's proximity to the equator. The peak incident irradiance during the summer solstice in June is 995 W/m^2, and 938 W/m^2 for the winter solstice. This comparison represents a difference of 6.08% between the two extremes of solar declination angle.

To model the expected power output for the Vieux Fort PV installation, it was also important to understand the effects of ambient temperature and local wind speed. These two environmental factors are significant drivers in the performance of any PV system, as they both have some effect on PV cell temperature. It is well known that an increase in PV cell temperature will result in diminished power output of the module. [16] The effect of cell temperature above standard test conditions (STC), affects the operating conditions of a PV module. Listed in Table 2 are the manufacturer provided temperature performance coefficients. [17]

The values presented in Table 2 represent the effect that cell temperature has on module performance, for temperatures exceeding the STC temperature of 25°C. Temperature derating is a critical design factor that must be accounted for, over the lifetime of a PV module. Minimizing the potential rise of cell temperature is best accomplished through structure design which permits cooling through wind convection. A rudimentary approach for estimating cell temperature is described in Equation 1.[16]

$$T_{cell} = T_{amb} + \left(\frac{NOCT - 20°C}{0.8 kW/m^2}\right).S\ (kW/m^2) \quad \text{(eq. 1)}$$

The above equation is considered an adequate method for predicting cell temperature rise. Equation 1 defines that cell temperature is only dependent on ambient temperature and solar irradiance incident onto the face of the PV collector. The range of ambient temperatures recorded in the

TMY data ranges from 25 °C to 30 °C. This range is relatively narrow considering that this range represents data collected during both night and day. Therefore, using only ambient air temperature and incident solar irradiance as means to estimating thermal derating of the PV module is likely to overestimate the performance of PV modules. By also accounting for convective cooling effects caused by ambient wind currents, a more accurate model of the thermal performance of the PV modules may be performed. This is not included in the present paper but is reported elsewhere [18].

B. Utility Wind Farm Site Selection

Like the Desruisseaux solar installation, the design of the Dennery wind farm is driven heavily by locality. The Dennery district is on the eastern side of Saint Lucia and is directly exposed to the Caribbean trade winds. The proposed location for wind turbine placement is located between two protected wildlife areas, and west of the town of Dennery.

This presents the challenge of finding suitable land, which is close to the end user, while not infringing upon either protected wildlife area. Further examination of the Dennery district depicts densely forested areas as being the only suitable locations for wind turbine installation. Since the challenge of foliage exists at all suitable locations, it is imperative to find site locations that have significant elevation. Wind power density is greatly dependent upon wind speed. If there are excessive impedances in the path of a wind current, the speed of the wind current is reduced. To mitigate this loss of speed, elevation of the point of wind power generation is crucial. Located in the Dennery district is an elevated region known as Morne Panache. The elevation of Morne Panache ranges between 200m and 300m above sea level. [13] The elevation of this region is ideal for wind power, since the wind impedance caused by surrounding tree coverage is reduced by the lower elevation located east of the proposed site. Additionally, there are two roads near this location, which can facilitate easier transportation of materials to the site. Figure 5 shows the defined location for wind turbine installation.

Figure 5: Potential Morne Panache Wind Power Site [13]

C. Dennery Wind Availability

Also, expressed by the NETS is the objective to install 12 MW of wind power onto Saint Lucia. The Dennery district on the eastern side of the island is ideal since there is consistent exposure to the Caribbean trade winds. The wind speed data presented in the TMY data set was sampled at a height of 10 meters. [15] To represent the estimated wind speed at the height of a wind turbine, it is necessary to adjust the 10 m height wind speed data to the equivalent height of the wind turbine.

Referencing the Tera Cora wind farm on Curaçao, lead to the selection of wind turbines manufactured by Vestas. This selection resulted in adjusting the wind speed to a height of 80 m, to represent wind present at the wind turbine hub. To adjust the wind speed data to a height of 80m, Equation 2 was utilized.

$$\left(\frac{v}{v_0}\right) = \left(\frac{H}{H_0}\right)^{\alpha} \qquad \text{(eq. 2)}$$

The variable (H) is chosen to represent the hub height of a Vestas brand wind turbine, 80 m. The wind friction coefficient (α) was chosen as the standard value of 1/7. [16] A Weibull probability density analysis of this height-adjusted wind speed data was performed. It is assumed that the wind speed data followed a Rayleigh distribution. Meaning that the applied shape factor for the Weibull distribution curve 'k' was equal to 2. Figures 6 and 7 illustrate the wind speed density curve for the two distinct seasons experienced by the region.

Initial examination of Figures 6 and 7 suggests the most probable wind speed is 6 m/s. However, the average wind speed for the dry season is 8.55 m/s, and a near equivalent 8.34 m/s for the wet season, due to the utilized Weibull probability density function. Following this data trend, it is clear the Dennery district is an advantageous location for utility-scale wind turbines. To accommodate wind speeds in this range, the Vestas V100-2.0MW wind turbine was selected. Shown below in Table 3 are relevant wind turbine specifications. Additionally, Figure 8 depicts the power curve for the V100-2.0MW turbine, with the assumption of standard air density.

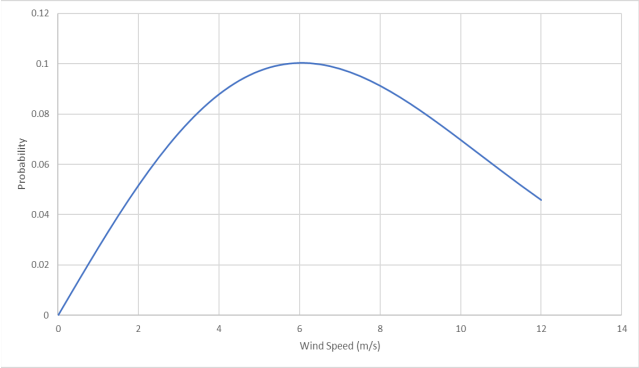

Figure 6: Dry Season Wind Speed Density Weibull Distribution

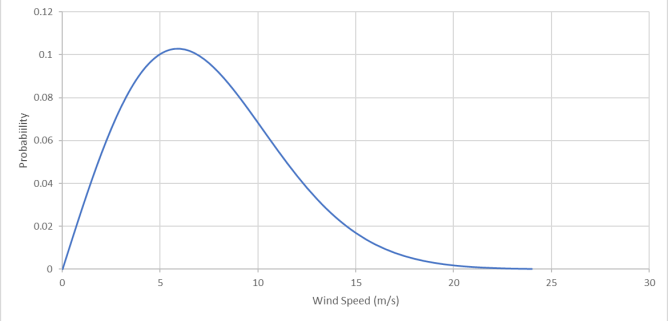

Figure 7: Wet Season Wind Speed Density Weibull Distribution

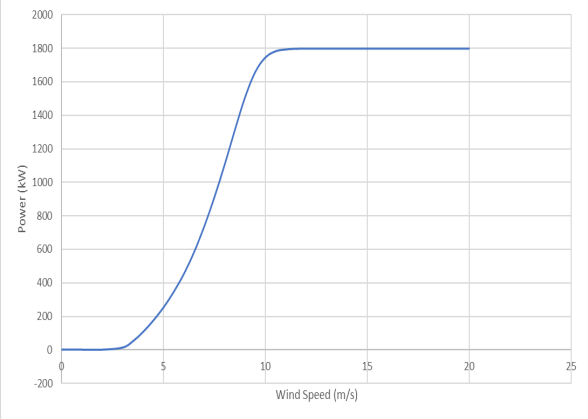

Figure 8: Vestas V100-2.0MW Power Curve
(Air Density = 1.225 kg/m^3)

To optimize wind power generation at Morne Panache, it is essential that adequate spacing between wind turbines is maintained. As stated earlier, upwind obstructions result in slower wind speeds further downstream. Therefore, an effort to align adjacent wind turbines with sufficient spacing is necessary. According to the recorded wind direction presented in the TMY data, for a significant majority of the year, the wind is blowing westward. Therefore, to minimize the impedance caused by adjacent wind turbines, it is advantageous to align the wind turbines in a straight line.

The minimal spacing between adjacent wind turbines is between 240m and 400m. [16] These distances are equivalent to 3 and 5 swept area diameters. Figure 9 illustrates the minimum spacing required between wind turbines. Figure 10 depicts the proposed locations of each wind turbine on a topographical map.

Table 3: Vestas V100-2.0MW Design Specifications [20]

Specification	Data Sheet Rating
Rated Apparent Power	2.0 MVA
Power Factor Range	0.90 Lagging – 0.95 Leading
Generator Type	Doubly-Fed Induction Generator
Generator Poles	4
Generator Voltage	690 VAC
Converter Voltage	480 VAC
Rated Frequency	50 Hz
Swept Area	7850 m^2
Rotor Speed Range	9.3 – 16.6 rpm
Cut-In Speed	3 m/s
Cut-Out Speed	22 m/s

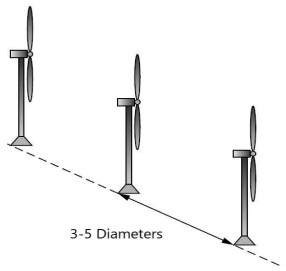

Figure 9: Wind Turbine Spacing [16] with each hub facing east.

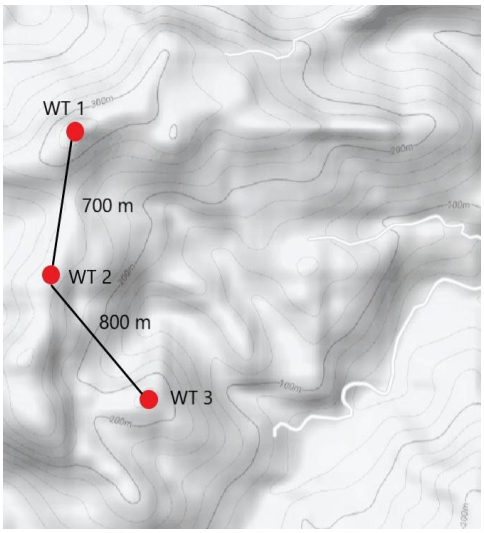

Figure 10: Topographical View of Morne Panache with Wind Turbine Spacing [13]

D. Desruisseaux Solar Array Design

The total available area at the location shown in Figure 20 is approximately 230,000 m^2. It was decided to utilize the exact design of the mounting structure for the PV modules at the Vieux Fort installation. The intent of this design decision is to maintain similarity between the two arrays to reduce tooling and maintenance cost across both installations. The configuration of the Vieux Fort PV module installation is shown in Figure 11.

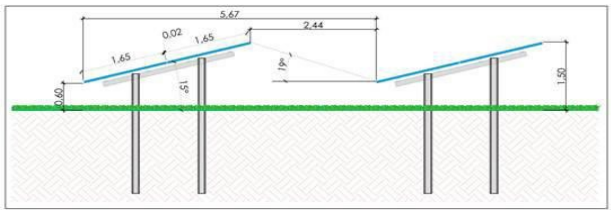

Figure 11: Vieux Fort PV Module Installation Configuration [19]

Additionally, like the Vieux Fort PV array, this Desruisseaux system will be rated for 1000 VDC. A nominal system voltage of 1000 VDC offers multiple benefits. The foremost advantage being the reduction of DC line losses. It is well known for all power distribution systems that relatively high voltages are best utilized when transmitting power between the point of generation and the point of use. By designing the Desruisseaux solar array to be rated for 1000 VDC, line losses will be reduced between the PV module and its associated power conversion equipment.

The PV module selected for this design was the TSM 245 DC-05, due to its relatively high efficiency and rated

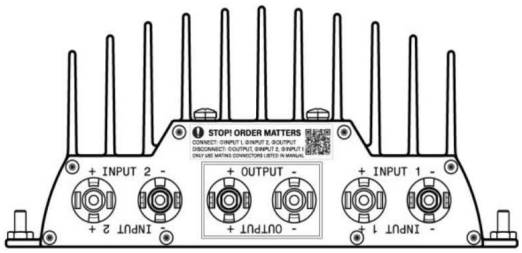

Figure 12: AMPT V900-32-32 String Optimizer

power. The module characteristics are provided in Table 4.

Based on the PV module design specifications listed in Table 5, the maximum permissible PV modules arranged in a serial configuration is 26 modules, which corresponds to a maximum open-circuit voltage of 970 VDC and maximum power voltage of 798 VDC. The term "string" will be utilized to reference a serial configuration of 26 PV modules. One design constraint with this system voltage is the insulation rating of the cable. In general, the cost of any cable will increase as its insulation rating increases. Power cable with an insulation rating of 600 V is widely available. To accommodate a 600V insulation rating, a common design practice is implemented. It is possible to subdivide a string of PV modules into two sub-strings. This is accomplished by setting the neutral point of a string, between two modules. [21] In this design, the neutral point of the system is chosen to be between the 13th and 14th PV

Table 4: TSM 245DC-05 Module Design Specifications [17]

Specification	Data Sheet Rating
Cell Type	Monocrystalline
Peak Power	245 WDC
Module Efficiency	15 %
Power Tolerance	3 %
Nominal Operating Cell Temp	46 °C
Maximum System Voltage	1000 V
Maximum Power Voltage	30.7 V
Maximum Power Current	7.98 A
Open Circuit Voltage	37.3 V
Short Circuit Current	8.47 A
Fill Factor	77.54 %
Dimensions	L 1650mm x W 992mm x D 46 mm

module in a 26- module string. This effectively creates two sub-strings each with a maximum voltage of ± 485 VDC. This design accommodates cabling with 600V insulation ratings, which leads to reduced cable cost. While also supplying 1000V-rated power to downstream power conversion equipment. The rated current for the TSM DC-05 245 PV module is 7.98 A. Therefore, the rated power of a

single string is approximately 6.37 kW. However, this rated power is calculated on the basis that 1000 W/m^2 irradiance is constantly available with no fluctuations. These fluctuations are commonly caused by shading from nearby obstructions or intermittent cloud coverage. To ensure that steady power is sourced from a PV string, it is necessary to integrate some form of output voltage regulation across a PV string.

Table 5: AMPT V900-32-32 Design Specifications

Specification	Rating
Maximum Voltage per Input	1000 VDC
Tracking Voltage Range per Input	300 – 770 VDC
Maximum Current per Input	24 ADC
Maximum Short Circuit Current Pet Input	26 ADC
Output Voltage Range	0 – 900 VDC
Output Voltage at Full Power	820 VDC
Open Circuit Voltage	900 VDC
Maximum Output Current	32 ADC
Continuous Power Rating	26.0 kW
Maximum Efficiency	99.4%

To regulate the output power of each PV string, a device which executes maximum power point tracking is critical. Without sufficient DC voltage regulation, downstream power conversion equipment, such as a centralized inverter, will be unable to convert power efficiently, due to a multitude of varied inputs. Therefore, by regulating a DC bus voltage near the point of power generation permits efficient power delivery to the grid. The specific MPPT device used in this design is the AMPT V900-32-32, shown in Figure 12 and its design specifications in Table 5. [22]

To best utilize the AMPT V900 string optimizer, it is important to ensure that its input is properly loaded. Comparison of the maximum power output current of the TSM DC-05 245 to the AMPT V900 input current yields that three PV strings should be connected in parallel. Through this parallel arrangement, the expected maximum input current per channel of the AMPT V900 is 23.94 ADC. This results in a total input power of 19.10 kW, assuming 1000W/m^2 of solar irradiance. Which yields an estimated output power of 18.9 kW per AMPT V900. Another useful facet of the AMPT V900 is the option to integrate a remote monitoring communications system, StringView. This communication system is capable of transmitting string-level data to a remote monitoring station with an accuracy of 0.25%. [23] This is an advantageous feature, as it enables the site operator to actively monitor partitions of the array and identify faults on the source-side of a string optimizer. In addition to StringView, series fuses for each string are installed with a rating of 10 A to protect the PV modules in the event of a ground fault. Other protection schemes such as insulation resistance monitoring were considered, but would result in higher design cost, device calibration cost, and maintenance periodicity. In turn, StringView and series fuses increase the reliability and maintainability of the entire PV system. The return side of the AMPT V900 output is grounded, in accordance with IEEE Standard 1547. [21] The outputs of each AMPT V900 are then routed through a series of combiner boxes towards a 1MW centralized inverter. The combiner boxes are also outfitted with circuit breakers for AMPT protection and isolation of specific partitions of the array. With a well-protected and monitored PV array, the centralized inverter can operate efficiently.

Figure 13 is the proposed design for the Desruisseaux solar installation. It is important to note that Figure 13 depicts the interconnection of a 1 MW portion of the array to a single 1 MW centralized inverter.

Table 6: Solar Ware 1000 Inverter Design Specifications

Specification	Rating
Maximum DC Voltage	1000 V DC
Maximum DC Current	1855 A DC
Nominal AC Power	3-Φ 1 MW / 1 MVA
Nominal AC Voltage	380 Vrms Δ
Nominal AC Current	1519 Arms
Power Factor Range	0.85 Lagging – 0.85 Leading
Operating Frequency	50 Hz
Maximum Efficiency	98.7%

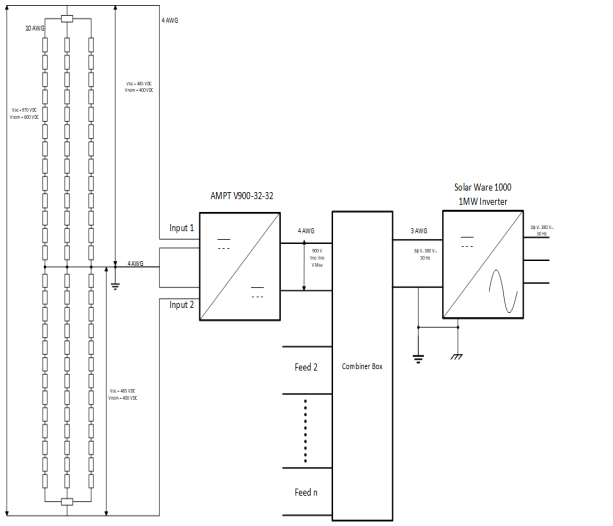

Figure 13: Proposed 1MW Interconnection of Desruisseaux Solar Installation

The proposed Desruisseaux solar installation is equipped with three 1MW centralized inverters. The selected inverter

is the Solar Ware 1000. This inverter is designed as a grid-following inverter, which prioritizes real power injection. The design specifications for this inverter are shown in Table 6. The one-line diagram of the Solar Ware 1000 Ware 1000 inverter is interfaced with its own 380 VLL / Inverter is shown in Figure 14.[24] The output of each Solar Ware 1000 inverter is interfaced with its own 380 VLL / 11kV kV 1.5 power transformers are interfaced to a MVA Δ-Δ transformer. The 11 kV secondary of these power transformers are interfaced to a common bus at the Desruisseaux solar installation. The opportunity to fully power the Praslin substation load solely generated power from this solar installation is routed by DERs and export excess power to the grid. The utilized directly to the Praslin substation. ETAP model is presented in Figure 15.

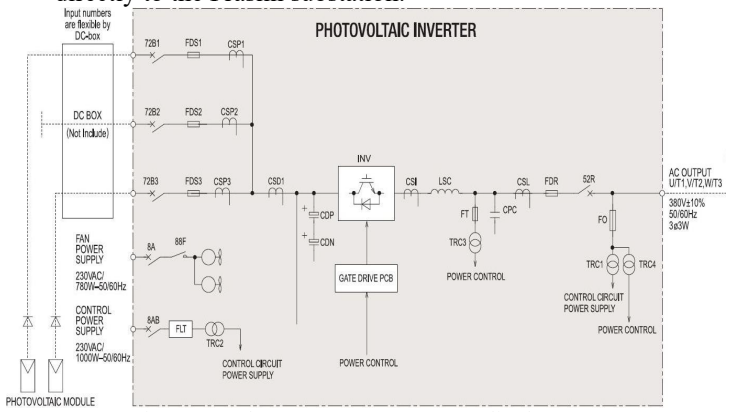

Figure 14: Solar Ware 1000 1 MW Centralized Inverter

III Model Derivation

A. *Praslin Substation with DER Integration*

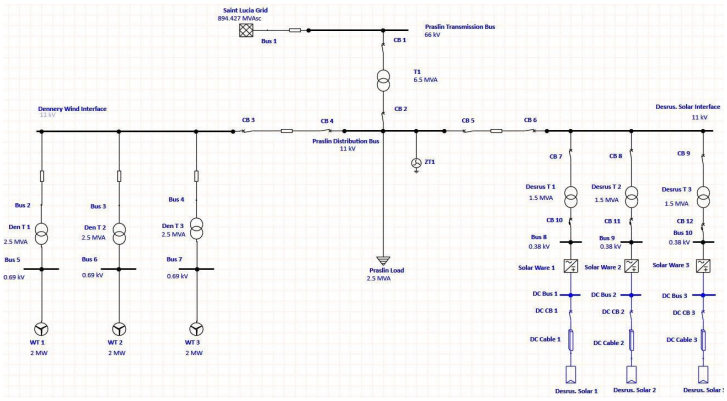

Figure 15: ETAP Model of Proposed Praslin Substation Integration of DERs

ETAP software was used to model DER integration into the electric grid of Saint Lucia. The primary intent of this simulation was to quantify the apparent power contribution from the proposed solar and wind DER installations. The site of DER integration is the Praslin substation, which houses a 6.5 MVA power transformer. [11] The Praslin substation is seen as an ideal location for immediate DER integration due to the peak load demand being relatively low at 2.5 MVA. [11] Due to this low peak demand, there is an opportunity to fully power the Praslin substation load solely by DERs and export excess power to the grid. The utilized ETAP model is presented in Figure 15.

The model presented in Figure 15 was utilized to quantify the apparent power contribution of each resource. Shown at the top of this model is the interconnection of the 66 kV transmission system with the 6.5 MVA Praslin substation transformer. The secondary of this transformer is connected to the main bus of the Praslin substation, which has a nominal voltage of 11 kV. The two proposed DERs interface onto the main bus of the Praslin substation through distribution cable. The left side of Figure 14 details the interface of the three Vestas V-100 wind turbines from Morne Panache. Each wind turbine output is interfaced with

Table 7: Praslin Substation Load (PF = 0.9 Lagging)

Hour	MVA	MW	MVAr
0.5	1.721	1.549	0.750
1.5	1.68	1.512	0.732
2.5	1.639	1.475	0.715
3.5	1.598	1.439	0.697
4.5	1.639	1.475	0.715
5.5	1.748	1.573	0.762
6.5	1.844	1.660	0.804
7.5	2.254	2.029	0.983
8.5	2.398	2.158	1.045
9.5	2.459	2.213	1.072
10.5	2.480	2.232	1.081
11.5	2.494	2.244	1.087
12.5	2.497	2.247	1.088
13.5	2.500	2.250	1.090
14.5	2.459	2.213	1.072
15.5	2.344	2.110	1.022
16.5	2.230	2.007	0.972
17.5	2.199	1.979	0.958
18.5	2.254	2.029	0.983
19.5	2.213	1.992	0.965
20.5	2.094	1.885	0.913
21.5	1.975	1.778	0.861
22.5	1.857	1.671	0.809
23.5	1.742	1.568	0.759

a 2.5 MVA transformer. The right side of Figure 14 depicts the interconnection of the Desruisseaux solar installation. Each 1 MW solar inverter is interfaced to a 1.5 MVA transformer. This model will compute the expected apparent power generation from each DER against the daily load profile of the Praslin substation shown in Table 7.

IV Results

A. Power Contribution of Sources

Two case scenarios were studied – a high renewables availability and a low renewables availability. The simulation results indicated that for both case scenarios considered, the integration of solar and wind DERs can fully support the load demand of the Praslin substation. Additionally, the combined generation of the two DERs is significantly greater than the Praslin load demand. In the low renewability resource case, Figure 16 shows the load demand, and the generation of solar and wind in the case of low renewable resource case. Figure 17 shows real and reactive power generation in the same case. In turn, this excess apparent power is supplied to the grid which should aid in reducing fuel consumption at CDSPS.

Figure 18 shows the load demand, and the generation of wind and solar in the case of high renewable resource availability. Figure 19 shows real and reactive power generation in the same case. Clearly, in both cases the load demand is met and both the real and reactive power is very significant, even in the case of low renewable energy resource availability.

Additionally, the combined generation of the two DERs is significantly greater than the Praslin load demand. In turn, this excess apparent power is supplied to the grid which should aid in reducing fuel consumption at CDSPS.

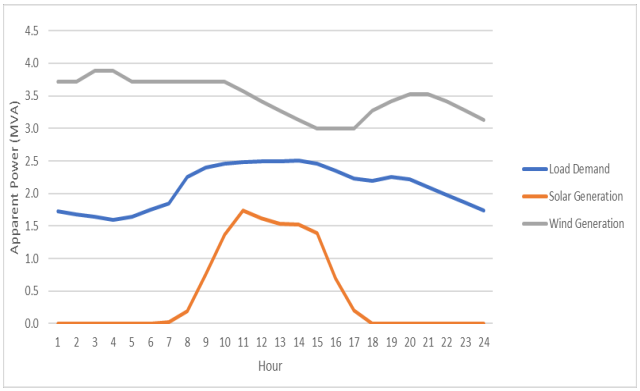

Figure 16: Low Renewable Resource Availability Generation and Demand

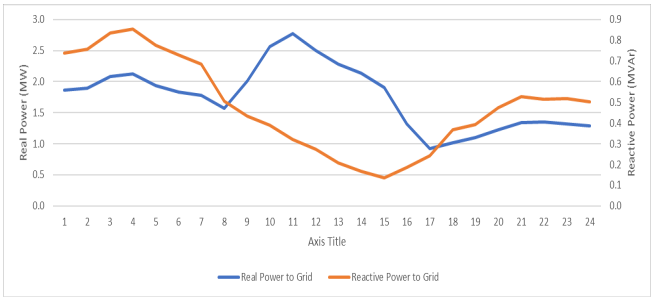

Figure 17: Low Renewable Resource Availability Grid Power Flow

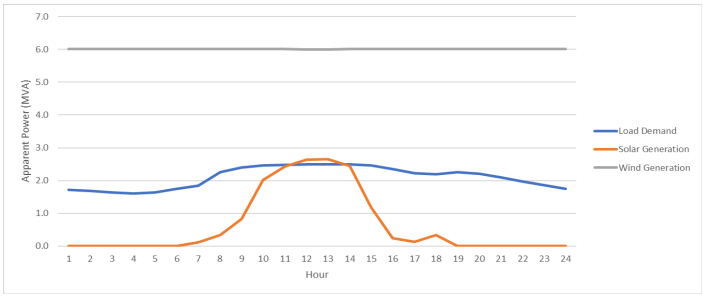

Figure 18: High Renewable Resource Availability Generation and Demand

Figure 19: High Renewable Resource Availability Grid Power Flow

V Conclusion

The current generation capability of CDSPS is nearing its firm capacity of 68 MW. If no other generation sources are brought online, it is expected that the firm capacity of CDSPS will be exceeded by 2026. The integration of the proposed solar and wind DERs can potentially increase firm capacity to 77 MW. Due to a steadily increasing annual load, near-term investment into DERs is highly advantageous. The climate and locality of Saint Lucia are ideal for solar and wind power resources, due to regularity in high insolation and wind speeds. In particular, wind-powered resources may prove more beneficial due to consistent exposure to moderate wind speeds. The steady state analysis performed via ETAP emphasizes both the necessity for DER integration, and intricacy of interfacing with the grid. This model can be modified to test different renewable resource availability and load profiles. From the

simulation results, power generated from DERs can supply the entirety of the Praslin district load, while also providing excess power to the grid.

From this investigation of Saint Lucia, a significant increase in renewable energy penetration is attainable. To take full advantage of the locality of Saint Lucia, further research into utility- interfaced energy storage is necessary. In particular, energy storage investment is crucial to improve grid reliability during outages, which would most likely occur during tropical storms. In general, further investigation and integration of more DERs onto the electric grid of Saint Lucia is advantageous, as it will reduce Saint Lucia's dependence on foreign fuel imports in accordance with its national energy transition strategy.

ACKNOWLEDGMENTS

The authors would like to thank Viviana Villavicencio Vallejo for her assistance with the modeling and simulation of the power grid using the ETAP software tool.

They would also like to express their appreciation to the engineers at Saint Lucia Electricity Services Limited (LUCELEC), especially Ormond Reece and Gilroy Pultie for providing details about the St. Lucia electric grid.

REFERENCES

[1] H. Ritchie, M. Roser and P. Rosado, "Energy Mix", *Our World in Data*, 2022. [Online]. Available: https://ourworldindata.org/energy-mix. [Accessed: 7-Feb-2022].

[2] The World Bank. 2020. *Population, total - St. Lucia | Data*. [online] Available at: https://data.worldbank.org/indicator/SP.POP.TOTL?locations=LC> [Accessed: 9-Feb-2022].

[3] The World Bank. 2018. *Surface Area - St. Lucia | Data*. [online] Available at: <https://data.worldbank.org/indicator/AG.SRF.TOTL.K2?locations=LC> [Accessed: 7-Feb-2022].

[4] The World Bank. 2018. *Terrestrial Protected Areas - St. Lucia | Data*. [online] Available at: <https://data.worldbank.org/indicator/ER.LND.PTLD.ZS?locations=LC> [Accessed: 7-Feb-2022].

[5] Central Intelligence Agency, "Saint Lucia", *Cia.gov*, 2022. [Online]. Available: https://www.cia.gov/the-world-factbook/countries/saint-lucia/#economy. [Accessed: 15-Jul-2022].

[6] World Trade Organization, 2020. *Saint Lucia Trade Profile*. [online] Wto.org. Available at: <https://www.wto.org/english/res_e/statis_e/daily_update_e/trade_profiles/LC_e.pdf>] [Accessed: 10-Feb-2022].

[7] LUCELEC, "Power Plants", *Lucelec.com*, 2022. [Online]. Available: https://www.lucelec.com/content/power-plants. [Accessed: 19-Jan-2022].

[8] LUCELEC, "Operations", *Lucelec.com*, 2022. [Online]. Available: https://www.lucelec.com/content/lucelecs-operations. [Accessed: 19-Jan-2022].

[9] Commonwealth of Saint Lucia, 2008. *Chapter 9.02 Electricity Supply Act.* Castries

[10] Saint Lucia Electricity Services Limited, "Saint Lucia National Energy Transition Strategy", LUCELEC, Castries, 2017.

[11] LUCELEC, "LUCELEC - 2021 Annual Report", *Lucelec.com*, 2022. [Online]. Available: https://www.lucelec.com/sites/default/files/annual-reports/LUCELEC%202021%20-%20Annual%20Report.pdf. [Accessed: 07-Jan- 2022].

[12] "LUCELEC officially opening Vieux Fort solar farm | Loop St. Lucia", *Loop News*, 2018. [Online]. Available: https://stlucia.loopnews.com/content/lucelec-officially- opening-vieux-fort-solar-farm. [Accessed: 09-Apr-2022].

[13] *Google Maps*. [Online]. Available: https://maps.google.com [Accessed: 20-May-2022].

[14] "Elevation Finder", *Free Map Tools*, 2022. [Online]. Available: https://www.freemaptools.com/elevation-finder.htm. [Accessed: 20-Feb-2022]

[15] "NSRDB Data Viewer", *Maps.nrel.gov*, 2022. [Online]. [Accessed: 15-Jan-2022].

[16] G. Masters, *Renewable and efficient electric power systems*. John Wiley & Sons Inc., 2013.

[17] Trina Solar, "TSM-DC05 Photovoltaic Module", 2022.

[18] P. Polselli, "Investigation and Implementation of Distributed Energy Resources onto the Island of St. Lucia", MS thesis, Villanova University, August 2022

[19] LUCELEC Representatives, 2022.

[20] Vestas, "General Specification V100-1.8/2.0 MW 50 Hz VCS", 2013.

[21] International Electrical and Electronics Engineers, "1547 - IEEE Standard for Interconnection and Interoperability of Distributed Energy Resources with Associated Electric Power Systems Interfaces", IEEE, New York City, 2018

[22] AMPT, "AMPT 1000-32-32 Series", 51770019-1 B, 2021.

[23] AMPT, "AMPT StringView", 2016

[24] Toshiba Mitsubishi-Electric Industrial Systems Corporation, "Solar Ware 1000", 2022.